

**Theory of Optical Processes in
Single-Walled Carbon Nanotubes**

by
Derek Van Orden

April 25, 2004

Theory of Optical Processes in Single-Walled Carbon Nanotubes

Abstract

Carbon nanotubes exhibit a variety of unique electrical, mechanical, magnetic, and optical properties that make them attractive for potential applications in nanotechnology. In this project the energy band structure of single-walled carbon nanotubes of arbitrary chirality is computed using a tight binding scheme that is generalized to include second nearest neighbor interactions. Plots of this band structure and the corresponding energy density of states may be used to predict the conduction properties of nanotubes, including the band-gaps of those exhibiting semiconductor behaviors, and the effective mass of electrons near the band edge. They may also be used to predict the energies of allowed optical transitions for incident light polarized along the tube axis as well as relative probability of observing each. Plots of the Brillouin zones in the reciprocal lattice give a qualitative explanation of the energy band structure. Finally, the model is modified to include the effect of a magnetic field parallel to the tube axis, which splits degenerate energy levels and narrows the band-gap between the valence and conduction bands. The amounts of splitting and band-gap reduction are dependent on the Aharonov-Bohm flux passing through the tube.

Table of Contents

I	Introduction	4
	- What nanotubes are, why they are important	
	- Research objectives	
	- Plot the band structure and the energy density of states	
	- Predict energies of allowed optical transitions	
	- Predict the effect of an external magnetic field	
	- Tube classification and chirality	
II	Background.....	5
	- Band structure calculations for planar graphite.	
	- Tight binding approximation	
	- Resulting two energy bands: conduction and valence	
	- Bloch's theorem and quantization of momentum	
III	Plotting Brillouin Zones of the Unit Cell in Momentum Space.....	7
	- Qualitative derivation of band structure and conduction properties	
	- Effects of trigonal warping in the reciprocal lattice.	
IV	Band Structure Calculations	11
	- Generalizing to tubes of arbitrary chirality	
	- Predicting allowed energy states	
	- Symmetry and asymmetry of energy states	
V	Density of States Calculation.....	14
	- General expression for one-dimensional density of states	
	- Combining the individual DOS corresponding to each allowed momentum state to plot a single density of states per unit length	
	- Problems of discontinuity and resolution	
VI	Including Magnetic Fields.....	18
	- Theory: Aharonov-Bohm effect and the addition of a phase factor	
	- Including it in the Band Structure program	
	- Results	
	- Splits degenerate states	
	- Decreases the band-gap	
VII	Including Second Nearest Neighbor Interactions.....	20
	- Formulation within tight-binding scheme	
	- Result: effect is apparently negligible for practical measurements	
VIII	Conclusion.....	22
	References.....	24

I. Introduction

The goal of this research project is to develop a reliable theory for calculating chirality dependent optical absorption and emission properties of single-walled carbon nanotubes. This theoretical model is based on band structure calculations, and is to incorporate second nearest neighbor interactions and the effect of a magnetic field parallel to the tube axis.

Single-walled carbon nanotubes are made from graphite sheets rolled up into seamless cylinders. As shown in Figure 1, the carbon atoms of a graphite sheet form a two-dimensional honeycomb lattice. There are an infinite number of different ways a tube can be rolled up. To quantify this, the vector that points along the tube circumference is called the chiral vector, and is denoted by $\vec{C} = n\mathbf{a}_1 + m\mathbf{a}_2$, where n and m are integers satisfying in $n \geq m$, and \mathbf{a}_1 and \mathbf{a}_2 are the primitive vectors in real space, shown in Figure 1. The chiral vector connects two crystallographically equivalent points on the graphene sheet (such as O and A in Fig. 1). Its magnitude is the tube's circumference. The translation vector \vec{T} (connecting O and B in Figure 1) is

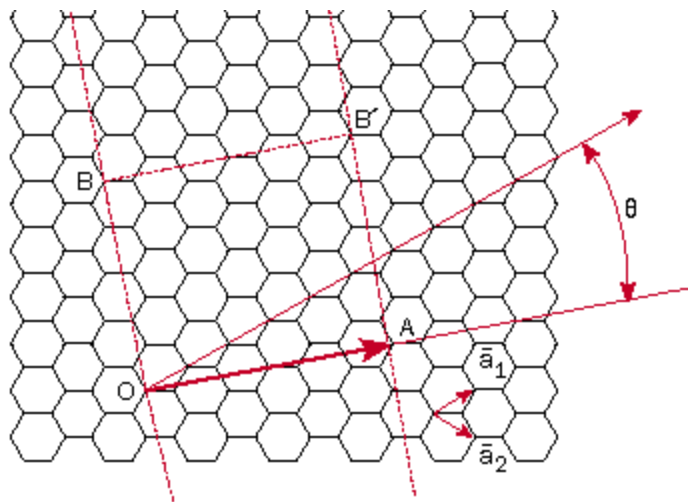


Figure 1:

The square AOB'B' defines the unit cell of a nanotube. The vector OA is the chiral vector given by

$$\vec{C} = n\mathbf{a}_1 + m\mathbf{a}_2$$

The angle θ it makes with \mathbf{a}_1 is called the chiral angle. OB is the translation vector \vec{T} , which points along the tube axis. [5]

perpendicular to it, and together the two define a rectangle that represents the unit cell of the tube, which repeats itself many times along the tube axis.

The index (n,m) is called the chirality of the tube. The electrical properties of carbon nanotubes depend strongly on their chirality. Some are semiconducting, whereas others are metallic. Some have only a few discrete energy subbands whereas others have hundreds. Because of this diversity, there is much interest in their potential applications, which include quantum wires and nanoscale transistors. Whether they are metallic or semiconducting, they always have extremely large aspect ratios; they generally have diameters ~ 1 nm, whereas their lengths can be larger than $100 \mu\text{m}$. They are much narrower and purer than any lithographically-fabricated semiconductor wires. This makes them ideal for the exploration of one-dimensional quantum physics.

II. Background

My first step was to write a program to plot the band structure of planar graphite. The calculations I used are based on the tight binding approximation, also known as linear combination of atomic orbitals. In this approximation the ground state energy of planar graphite is estimated using the variational method, in which the trial wavefunction is a superposition of the P_z orbital of a carbon atom and those of its three nearest neighbors. The coefficients of each term are found by minimizing the ground state energy. It can be shown that the contribution of the sigma orbitals becomes important only at very high energies, so here they are ignored; we are interested in lowest-energy interband transitions that typically occur in the near-infrared (~ 1 eV). With this formulation the energy is given by

$$E = \pm \frac{t \cdot f(k)}{1 \pm s \cdot f(k)} \quad (1)$$

where $f(k) = \pm[1 + 4 \cos(\sqrt{3}k_x a / 2) \cos(k_y a / 2) + \cos^2(k_y a / 2)]^{1/2}$

$$t = \langle \varphi(r) | \hat{H} | \varphi(r \pm a / 2) \rangle \quad \text{and} \quad s = \langle \varphi(r) | \varphi(r \pm a / 2) \rangle$$

where a is the lattice constant, about 1.42 angstroms, and $\varphi(r)$ is the wavefunction of the P_z orbital. t represents the transfer integral between this function and that of its nearest neighbor. It must be found experimentally, as the Hamiltonian is unknown, and the best known value is -2.7 eV for graphite. s is an overlap integral that is generally small enough to be neglected. It does not, in fact, have any effect on the energies of allowed optical transitions. This model ignores the effects of curvature, and so it is expected to work best for tubes whose diameters are large compared to the lattice constant. In all of these calculations the energy at each carbon atom is (arbitrarily) set equal to zero; only differences in energy need be considered to determine optical properties.

As it turns out, the reciprocal lattice of a graphite sheet is also a honeycomb lattice, though oriented differently. The first Brillouin zone is inside the hexagon around the origin (0,0), or the gamma point. All allowed states are contained inside within it. The six high-symmetry points at the zone boundary are called K points; the midpoint of two neighboring K points is called the M point, and the center of each hexagon (Brillouin zone) is the gamma point.

Figure 2 is a plot of this equation. It shows that the result is two energy bands, a conduction band and a valence band. They are symmetric only because the overlap integral s in equation (1) has been neglected. They are degenerate at the K points but

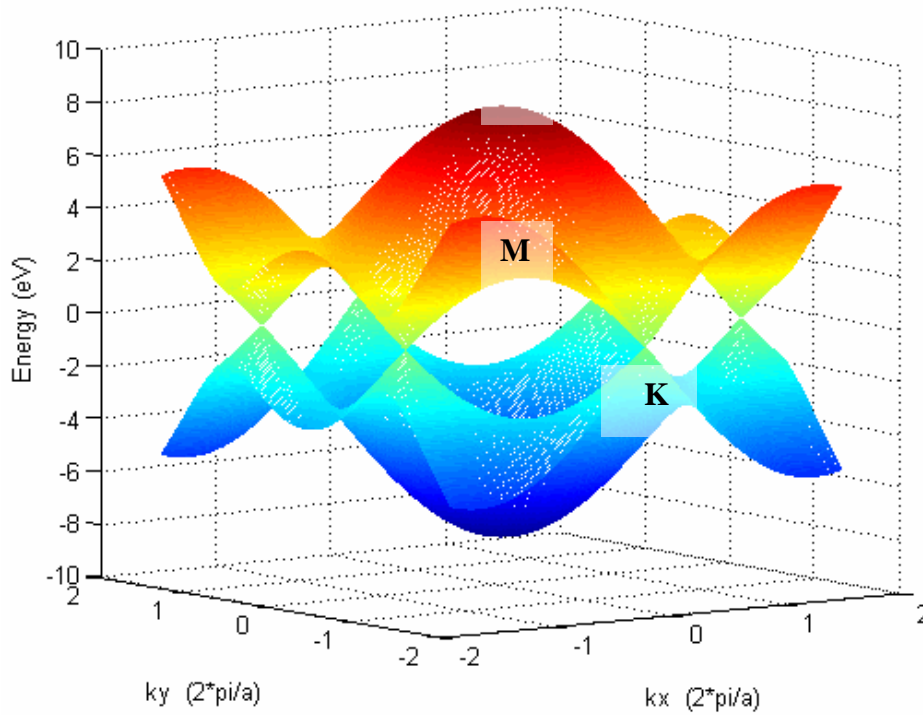


Figure 2:

A plot of the band structure of an infinite graphite plane in reciprocal space. Note that the two bands are degenerate at the K points

there is no overlap, so a graphene sheet is a zero-gap semiconductor. **Figure 3** is a plot of the energy contours of a single Brillouin zone. At the center these contours, on which the energy is constant, are circular, but close to the K points the asymmetry become more significant. This is responsible for a phenomenon known as trigonal warping, in which the contours become triangular.

The specialization of this calculation to nanotubes involves imposing upon the wavefunction periodic boundary conditions in the circumferential direction. Because the system is a crystal lattice, the wavefunction must obey Bloch's theorem:

$$\psi(\vec{r}) = \exp(i\vec{k} \cdot \vec{r}) \cdot u(\vec{r}) \quad (2)$$

That is, it can be expressed as a product of a function $u(\vec{r})$ that has the periodicity of the lattice and a modulating plane wave that generally does not. Therefore the boundary condition affects only the plane wave part. Requiring it to be invariant to translations

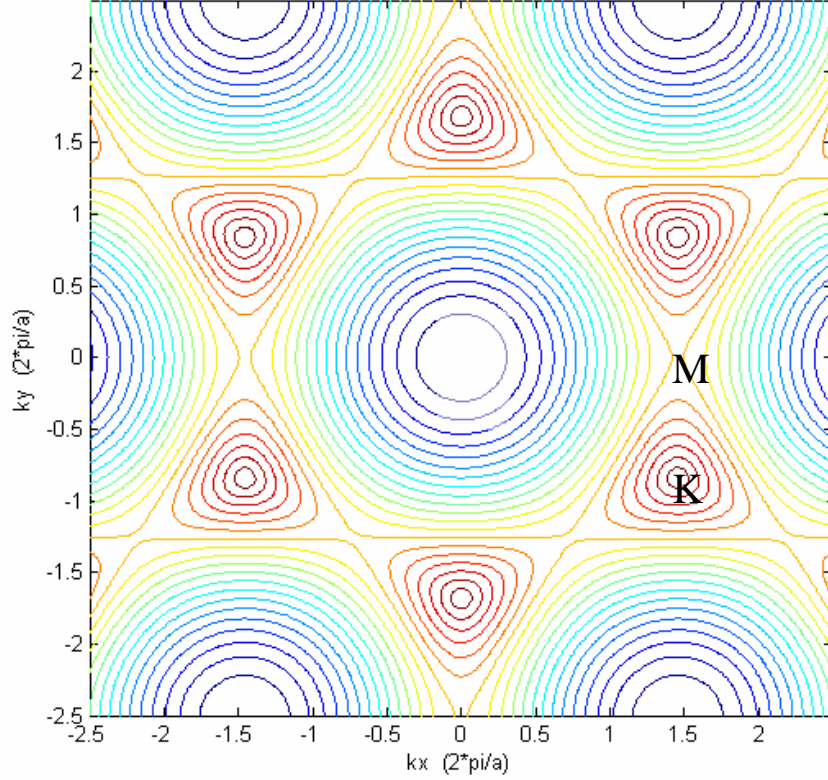


Figure 3:

Energy contours of the conduction band of planar graphite. Near the gamma point the contours are circular, but closer to the K points they become hexagonal, then triangular.

around the circumference gives a discrete number of allowed wave numbers.

$$\psi(\vec{r} + \vec{C}) = \exp(i\vec{k} \cdot \vec{r}) \cdot \exp(i\vec{k} \cdot \vec{C})u(\vec{r}) = \psi(\vec{r}) \quad \text{or} \quad k_c C = 2\pi\mu \quad \mu = 0,1,2\dots \quad (3)$$

where \vec{C} is the chiral vector that defines the circumference and k_c is proportional to the component of momentum in this direction. This discretization in turn gives the allowed energy levels of electrons in the tube through Equation (1). The length of a nanotube is on the order of a thousand times or more longer than its diameter, so the wave number (or momentum) in the axial direction can be well approximated as continuous. The calculation therefore assumes a tube of infinite length.

Plotting the band structure for a tube of arbitrary chirality then requires a translation of Equation (1) to a new basis defined in terms of the reciprocal chiral and translation vectors, \vec{K}_1 and \vec{K}_2 respectively, which are found by requiring that

$$\vec{C} \cdot \vec{K}_1 = 2\pi \quad \text{and} \quad \vec{T} \cdot \vec{K}_2 = 2\pi \quad (4)$$

The result is
$$(k_x, k_y) = k \cdot \hat{K}_2 + \mu \cdot \vec{K}_1 \quad (5)$$

where k gives the momentum along the tube axis and \hat{K}_2 is the reciprocal translation vector normalized to unity. Here the momentum quantization along the circumference found in Equation (3) is included. This change is necessary because these two vectors represent, in momentum space, the directions along which the wave number is discrete and continuous, and are therefore the only directions of interest.

III. Plotting Brillouin Zones

To gain a qualitative understanding of the energy properties of nanotubes, it is instructive to view the Brillouin zones of the allowed electron states in the reciprocal lattice. **Figure 4** shows this for an (8,8) tube. The line segments show the allowed momentum values an electron may assume. The first and last segments are in fact the same zone; it is plotted twice at each end to emphasize the periodic nature of the lattice. At any point in one of these zones an electron may assume one of two energy levels, one in each of the conduction and valence bands.

The MatLab program I wrote to make this plot uses the `gplot` command to construct the reciprocal lattice by specifying nodes (K points) and the connections between them. The dashed black line traces the reciprocal chiral vector. In this direction only discrete wave numbers are allowed. In the axial (vertical) direction there is no such quantization. At the end of each segment shown the Brillouin zone repeats itself along the axis.

In the (8,8) tube one of the 16 Brillouin zones intersects a K point. Since this is the point where the conduction and valence bands meet, one can see that the band-gap

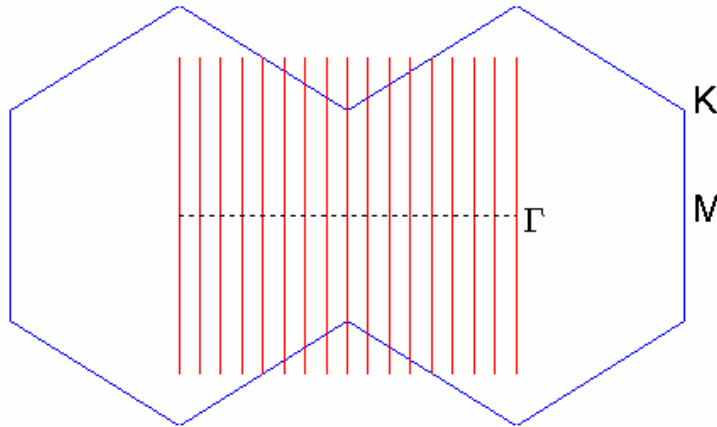


Figure 4:

The Brillouin zones of a (8,8) nanotube in the reciprocal lattice. Because one of them intersects a K point, the tube has a zero band-gap.

must be zero. The tube is expected to be metallic, provided that the density of states (DOS) at the Fermi energy (E_F , the energy of the highest allowed state at absolute zero) is not zero. A determination of this will require DOD calculations, and is presented in Section V. Figure 5, in contrast, shows the momentum states of a (5,0) tube. In this case there are only 10 different Brillouin zones, none of which cross a K point. This tube has a finite band-gap and will be semiconducting if the Fermi energy lies within this band-gap.

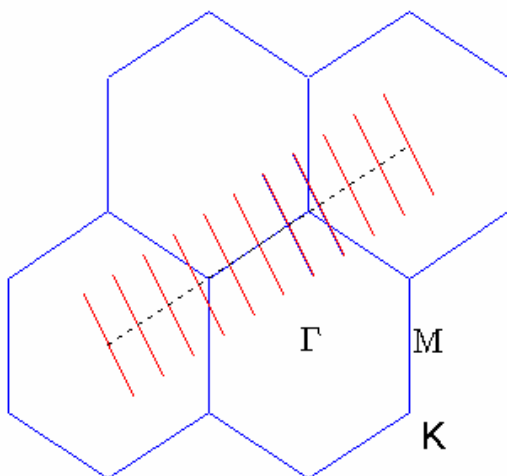


Figure 5

The Brillouin zones of a (5,0) nanotube in the reciprocal lattice. Because none of them intersects a lattice point, the tube is expected to have a nonzero band-gap.

IV. Band Structure Calculations

Although these plots are instructive, quantitative predictions would be more useful. I wrote another program to do this by plotting all the possible energies over the span of a single Brillouin zone. This allows one to predict the band-gap and the energies of allowed optical transitions.

Figure 6 shows the energy structure of a (8,8) tube. It plots Equation (1) over a single Brillouin zone for every allowed value of (k_x, k_y) as given by Equation (5), where k , the wave-vector in the direction of the reciprocal translation vector, ranges from $-\pi/|\vec{T}|$ to $\pi/|\vec{T}|$, or across the unit cell. The upper curves represent the conduction band whereas the lower ones make up the valence band. Curves that are symmetric represent states that have the same momentum along the circumference- this originates from the plus/minus sign in the original energy expression for planar graphite. (This mirror symmetry between the conduction and valence bands arises only through the neglect of the overlap integral s in Equation (1)). The two middle curves meet at zero energy at two points, so there is no band-gap. These two points represent the two K points intersected by the central Brillouin zone shown in Figure 4, the points at which the conduction and valence bands are degenerate.

Another interesting feature is the kink in these two curves at each K point. To understand the origin of this, one must refer back to Figures 2 and 3. Close examination reveals that in planar graphite the energy bands do indeed have a kink at the lattice point, where the dispersion becomes nearly linear, but with a different slope in each direction. The unusual shape is therefore not unexpected.

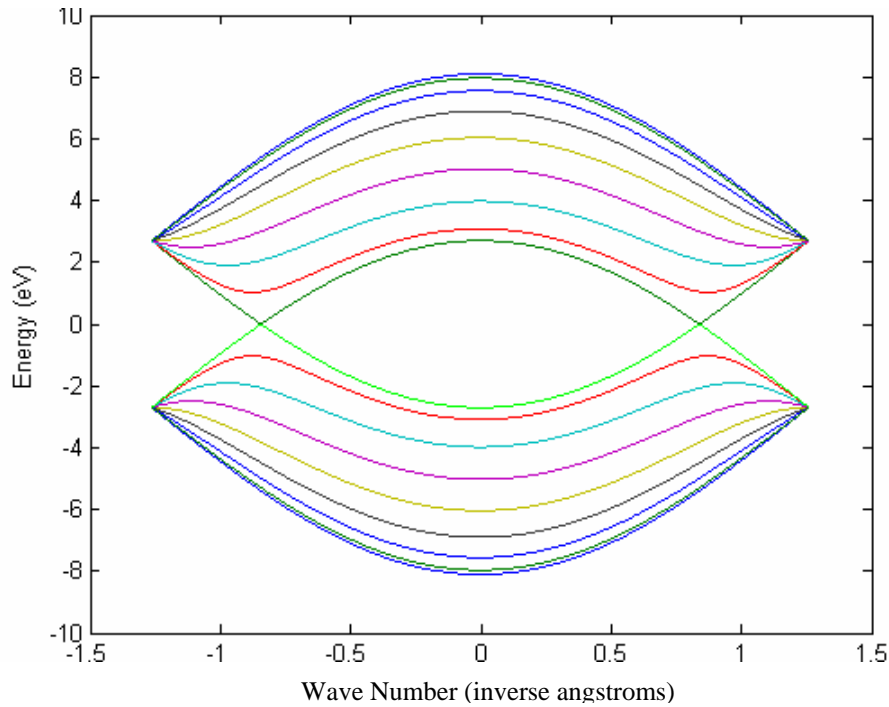


Figure 6

Band structure of a (8,8) nanotube. The intersection of the two bands at the K point results in a zero band-gap. Notice the kink in the two center curves where they meet at zero energy.

Note also that whereas Figure 4 shows 16 Brillouin zones, Figure 6 has only 9 curves (or subbands) in each band. This indicates that there must be high degeneracy. As it turns out, there are 7 doubly degenerate energy levels. This simply reflects the symmetry of the system. In Figure 4 all the Brillouin zones except the ones at the gamma point and the K point have a “mirror image” placed in an identical part of the reciprocal lattice but on the other side of the central zone, so they have identical band structures.

Figure 7 shows the band structure of the (5,0) tube. It shows high degeneracy as well; there are only 6 subbands for the 10 Brillouin zones shown in Figure 5. Because there are no allowed states in the central energy region, this tube has a finite band-gap, as predicted by Figure 5. One can see it is 2.06 eV.

These tubes both have symmetric energy band structures: that is, they are invariant to reflection about the $k = 0$ line. This can be understood qualitatively by

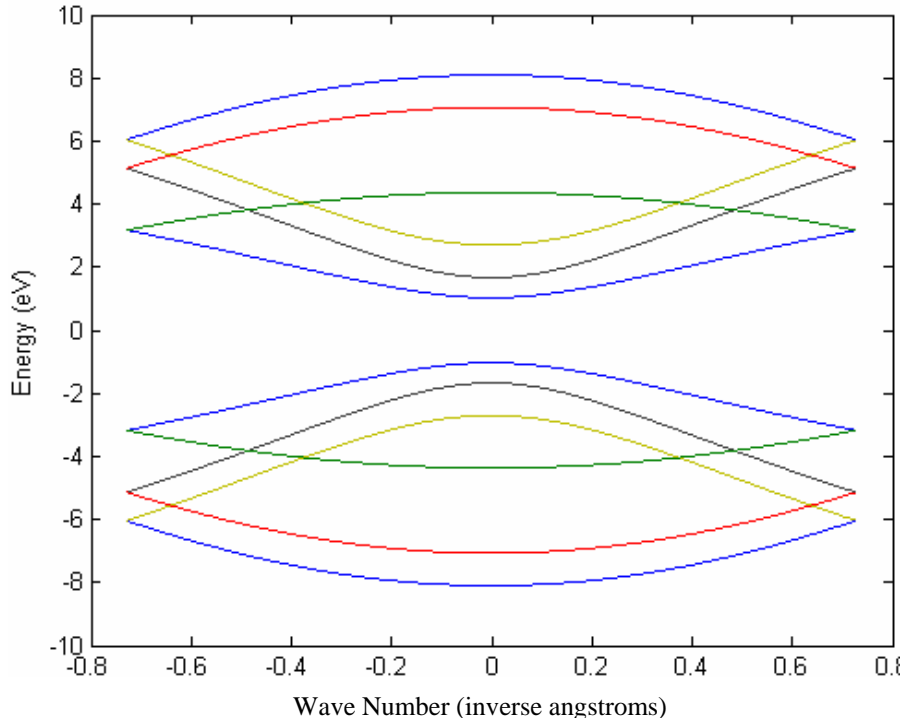


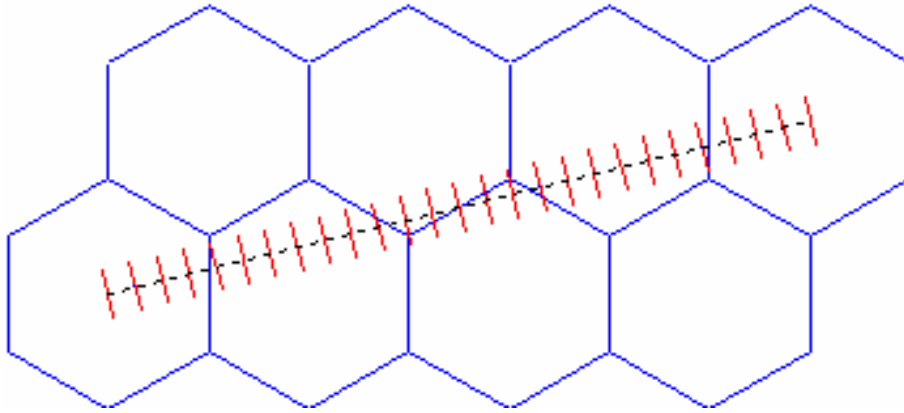
Figure 7

Band structure of a (5,0) nanotube. The two bands never intersect, so the tube is semiconducting.

examining the chiral indices. For an “armchair” tube, in which $m = 0$, the chiral angle is zero. For a “zigzag” tube, in which $m = n$, the chiral angle is 30 degrees, so that the tube is simply rolled up along the x-axis. Figures 4 and 5 show that in these cases the reciprocal chiral vector defines a line of symmetry in momentum space (shown as a dashed black line). No other chiral angles can produce this reflection invariance.

Tubes whose chiral indices satisfy neither of these criteria are called chiral tubes, and the energy bands do not exhibit this property. Figure 8 shows the Brillouin zones of a (5,2) chiral tube. One can clearly see that they do not have reflection symmetry about a center zone. However, close inspection reveals that they form anti-symmetric pairs: each occupies the same spot in the reciprocal lattice as its “mirror image” about the central Brillouin zone, except that it is reflected about its perpendicular bisector. This results from the fact that this line, which coincides with the reciprocal chiral vector, is not a line of symmetry as it is for armchair and zigzag nanotubes.

Figure 8: The Brillouin zones of a (5,2) chiral tube. Note the lack of inversion symmetry about the dashed line defined by the reciprocal chiral vector, and the anti-symmetric pairs of Brillouin zones, such as the two that intersect a K point.



One of the consequences of this is that in dispersion plots the individual energy subbands are not symmetric about $k = 0$, as shown in Figure 9 for the (5,2) tube. Hence, there is no degeneracy. Each one, however, has a mirror image about this line so that the overall dispersion is symmetric. Also, some of the energy curves are linear. This results from the fact that some of the Brillouin zones near the K point are found within the triangular energy contours shown in Figure 3, where the dispersion becomes linear.

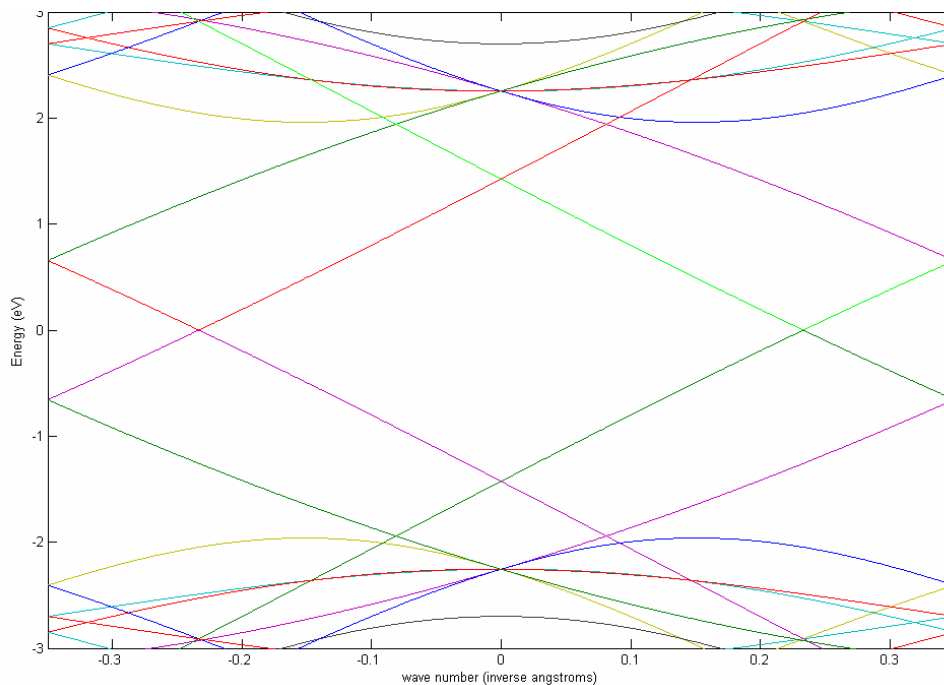


Figure 9

Detail of the dispersion of a (5,2) chiral nanotube. Note the asymmetry of individual subbands about the $k = 0$ line, but the overall symmetry resulting from the presence of corresponding anti-symmetric, or mirror image subbands. There are a total of 124 subbands in each of the conduction and valance bands.

V. Density of States Calculation

Of particular interest when researching optical properties is the energy density of states, or DOS, which gives the number of states in each infinitesimal increment $[E, E + dE]$ of energy. This reveals how many different transitions contribute to a particular transition with a particular energy, and this, together with the dipole matrix element between the initial and final states, determines the strength of that transition. At band extrema, the DOS exhibits kinks (in 3-D), steps (in 2-D), and peaks (in 1-D), and these are known as van Hove singularities. The 1-D van Hove peaks are important in determining interband optical properties, though in practice experiments show they are replaced in nanotubes by peaks associated with exciton transitions. The distance between peaks gives the energy of the optical transitions that are most likely to be observed, and their size can be used to predict the relative transition probability of each. In one dimension the expression for the DOS per unit length is

$$g(E) = \left| \frac{2}{\pi} \cdot \left(\frac{dE}{dk} \right)^{-1} \right| \quad (6)$$

The peaks occur at the extrema of the dispersion plots. My program can thus calculate the energies of each transition associated with these van Hove singularities by finding the points in the conduction band at which the derivative dE/dk goes to zero, then subtracting the energy of the corresponding point in the valence band. I calculated the expression for the DOS using Equation (1) to be

$$g(E) = \left| \frac{2 \cdot E \cdot |\vec{K}_2|}{\pi \cdot a} \cdot \left(K_{2y} \cdot [\cos(\alpha) \cos(\beta) + \sin(2\beta)] + \sqrt{3} K_{2x} \sin(\alpha) \cos(\beta) \right)^{-1} \right|$$

where

$$\alpha = \frac{a \cdot \sqrt{3}}{2} \cdot \left(\frac{K_{2x}}{|\vec{K}_2|} \cdot k + \mu \cdot K_{1x} \right) \quad \text{and} \quad \beta = \frac{a}{2} \cdot \left(\frac{K_{2y}}{|\vec{K}_2|} \cdot k + \mu \cdot K_{1y} \right) \quad (7)$$

It is easily shown that at the K point both the energy E and the denominator are identically zero, so the derivative at this point does not exist, in agreement with the kinked curve in Figure 6. To account for this, my program also finds any discontinuities in the derivative and considers them as critical points for transition energy calculations. Though the derivative is not continuous, its absolute value is; because of the symmetry of the band structure near the K point, the dispersion curves approach it at the same angle from opposite directions. The density of states is defined and is nonzero at this point.

Each energy subband has a van Hove singularity in the energy range in which an electron is most likely to be observed. To find the total DOS these must be summed over all possible values of μ in Equation (3) (i.e., over all subbands). Computationally this was somewhat challenging because the DOS depends on the wave number, so one cannot simply calculate and sum it for each value of energy. I had to calculate the DOS for every value of k , then, to relate it to the energy, find and average the values of it in each of a number of small increments that divided the energy range. If the incrementation were too small, some increments would have no points, so the plot would go to zero and have many kinks. If it were too large the plot would have poor resolution. By trial and error, I found that a good compromise was to divide the allowed energy range into a hundred different regions for ten times as many k values, so that on average one would find ten points per interval.

Figure 10 shows the DOS per unit length of the (5,0) nanotube. The region in the middle, where an electron has no probability of being found, represents the band-gap.

Because the Fermi energy lies within the band-gap, this tube is a semiconductor. This feature does not appear in the plot of the DOS for the (8,8) tube shown in Figure 11; the DOS is nonzero at the Fermi energy, so this tube is expected to exhibit metallic properties, the band-gap being zero. There are 12 singularities in each band, one for each of the 9 energy curves in Figure 6, and one more for each of those with an additional critical point near the K point.

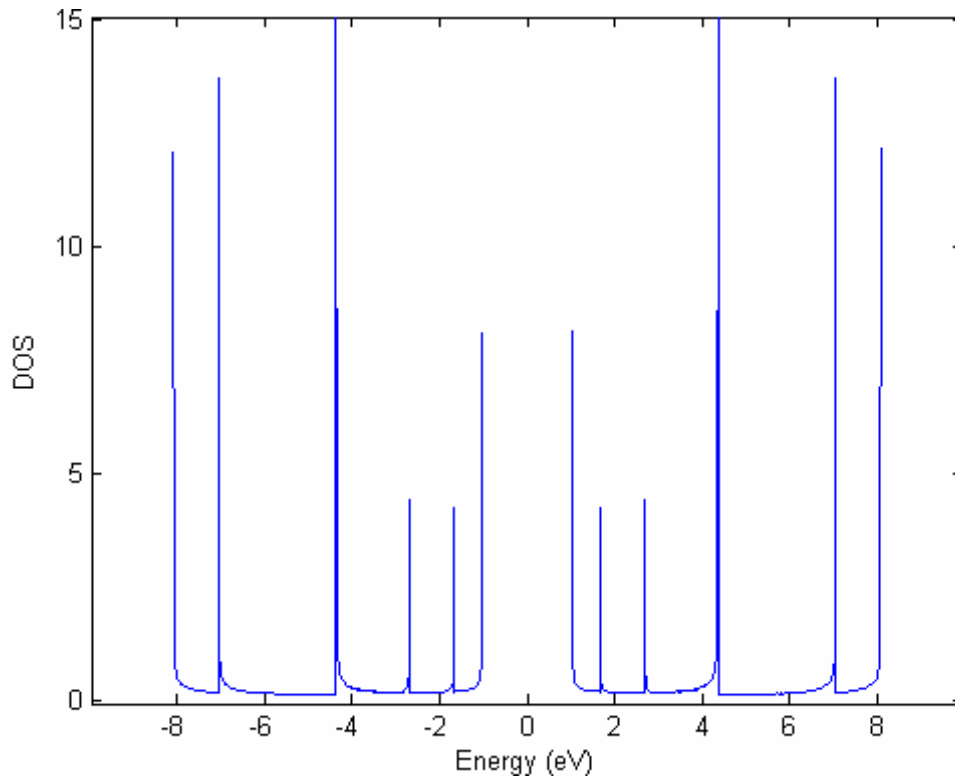


Figure 10
DOS for the (5,0) tube. The 6 peaks in each band correspond to the six energy curves shown in Fig 7. For light polarized along the tube axis, optical transitions may occur only between mirror image spikes.

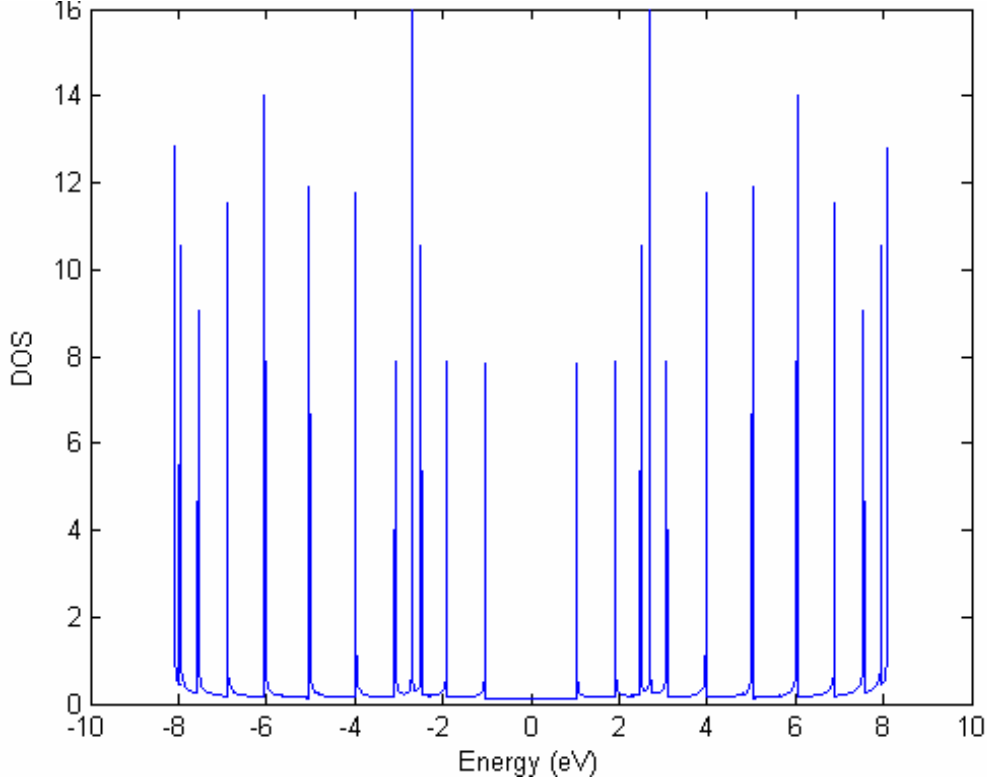


Figure 11

DOS for the (8,8) tube. The 12 peaks in each band correspond to the 12 critical points of energy subband curves shown in Fig 6.

VI. Including Magnetic Fields

Next I set out to find the effect of an external magnetic field parallel to the nanotube axis on the energy band structure. First I tried to calculate the change in momentum due to the Lorenz force acting on the electrons. I found

$$\vec{k} \Rightarrow \vec{k} + \frac{e}{\hbar} \cdot \vec{A} = \vec{k} + \frac{e}{2\hbar} \cdot \vec{r} \times \vec{B} \quad (8)$$

where \vec{r} is the position on the tube surface, $\vec{B} = B \cdot \hat{z}$ is the magnetic field, and \vec{A} is its vector potential. Then Equation (3) becomes

$$\left(\vec{k} + \frac{e}{2\hbar} \cdot \vec{r} \times \vec{B} \right) \cdot \vec{C} = 2\pi\mu \quad (9)$$

However,
$$(\vec{r} \times \vec{B}) \cdot \vec{C} = (\vec{C} \times \vec{r}) \cdot \vec{B} = 0 \quad (10)$$

because in curvilinear coordinates both \vec{C} and \vec{r} lie in a plane parallel to the magnetic field. The expression for momentum quantization remains unchanged.

This does not, however, mean that there is no change in the energy structure. One must also consider a purely quantum phenomenon known as the Aharonov-Bohm effect. This adds a phase factor to the wave number in the axial direction that is proportional to the magnetic flux passing through the tube. The expression for the wave number becomes

$$\vec{K}_1 \Rightarrow \vec{K}_1 + \frac{\phi}{C \cdot \phi_0} \quad \text{where } \phi_0 = \frac{h}{e} \quad (11)$$

Here ϕ is the magnetic flux passing through the tube, h is Planck's constant, and e is the elementary charge. C , the magnitude of the chiral vector, is simply the tube's circumference. One can see that the effect is to translate the Brillouin zones along their perpendicular bisector in the reciprocal lattice. Equivalently, one may view the field as changing the momentum quantization condition in Equation (3) to

$$k_c C + \frac{\phi}{\phi_0} = 2\pi\mu \quad (12)$$

In either case, one can see that it will make conducting tubes slightly semiconducting by moving the Brillouin zone off the K point in the reciprocal lattice. For tubes that are already semiconducting it will narrow the band-gap, as the Brillouin zones are shifted closer to the K points. Because the flux is proportional to the tube's diameter, these effects will be much more important for larger tubes. Figure 12 shows the reciprocal lattice of the (10,2) tube with a 45 Tesla magnetic field pointing along its axis. The red segments indicate the Brillouin zones without an external field and the blue segments show the shift caused by applying one. The small spacing between each of the 124

Brillouin zones makes this translation relatively large. The field causes the band-gap of this tube to fall 18 meV.

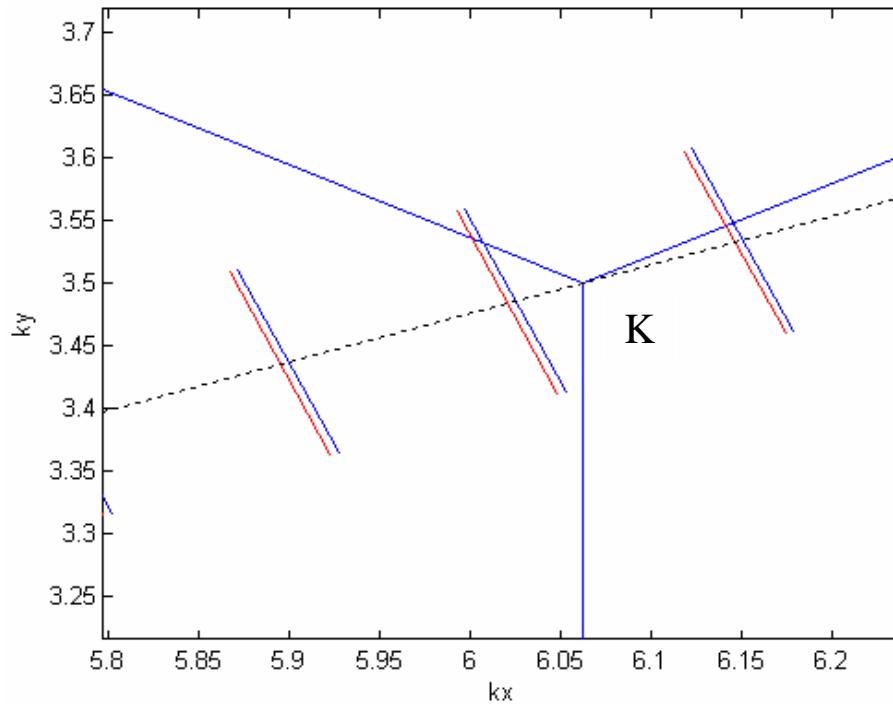


Figure 12

The shift of the Brillouin zones from their positions at 0 Tesla (red) to their new positions at 45 Tesla (blue) near a K point of a (10,2) nanotube. The dotted black line shows the direction of the reciprocal chiral vector.

I have shown in Figure 13 the band structure of an (8,8) tube in a very high field of 1000 T so that the effects are strong enough to be seen graphically. Compared to Figure 6, one observes here that the tube is no longer metallic. It is a semiconductor with a band gap of 0.53 eV. Furthermore, 16 energy curves can be distinguished in each band, showing that all the degeneracy has been lifted, or that the shift of Brillouin zones has broken their reflection symmetry about the center zone that is displayed in Figure 4.

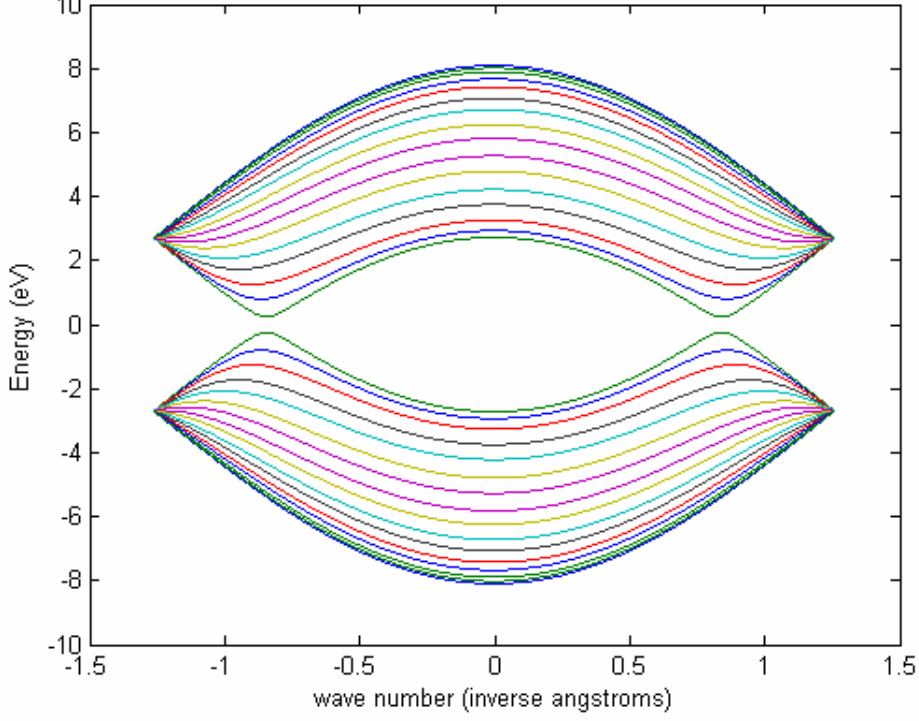


Figure 12

The band structure of an (8,8) nanotube in the presence of a 1000 T magnetic field pointing along its axis. Note that the tube now has a finite band-gap and that all degenerate levels have been split. Compare with Figure 6, which shows the dispersion in zero magnetic field.

VII. Second Nearest Neighbor Interactions

The expression for the energy in Equation (1) is based on a tight binding scheme that includes only the nearest neighbor interactions. Extending this calculation to second nearest neighbors would presumably give a more accurate expression. I found the general equation to be

$$\begin{aligned}
 E(\vec{k}) = & \pm t \cdot \sqrt{1 + 4 \cos(\sqrt{3}k_x a/2) \cos(k_y a/2) + \cos^2(k_y a/2)} + \\
 & 2 \cdot t' \cdot [\cos([\sqrt{3}k_x + k_y]a/2) + \cos([\sqrt{3}k_x - k_y]a/2) + \cos(a \cdot k_y)] \quad (13) \\
 t' = & \langle \varphi(r) | \hat{H} | \varphi(r \pm a) \rangle
 \end{aligned}$$

where t' , another transfer integral, is equal to -0.073eV [5].

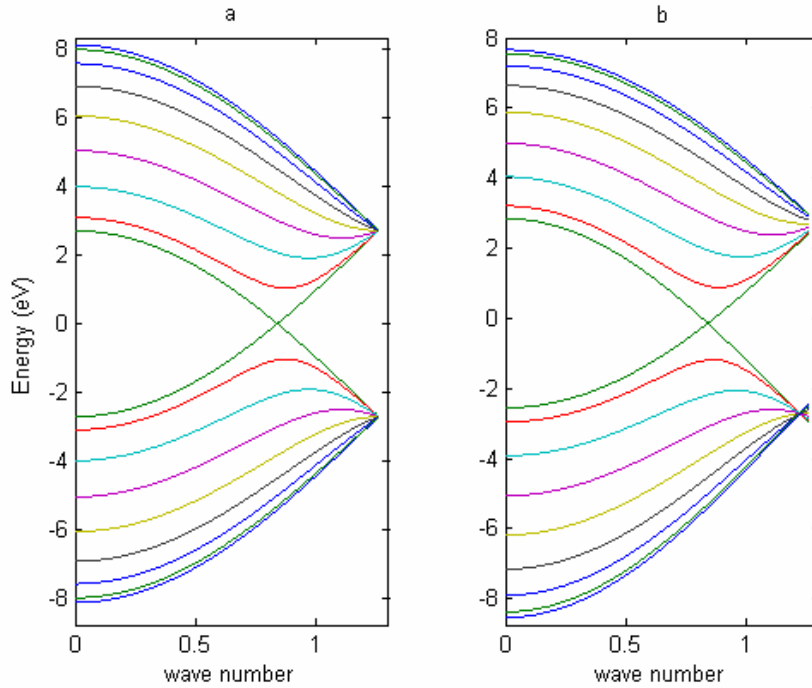


Figure 13

- (a) Dispersion plot for a (8,8) tube including only nearest neighbor interactions.
- (b) Dispersion plot for a (8,8) tube including second nearest neighbor interactions as well.

Because the momentum quantization condition Equation (3) is unaffected by this change, the placement of the Brillouin zones is also unaffected. Their symmetry, and thus the degeneracies are all preserved. One can see in Figure 13 that the result is a slight broadening of the valence band and a narrowing of the conduction bands; the two energy bands become asymmetric, though this asymmetry is negligible compared to that introduced by the overlap integral s in Equation (1). As it turns out, the inclusion of this extra term changes the energy transitions very little; on the order of less than 1 meV, so in fact the exclusion of next nearest neighbor interactions is justified.

VIII. Conclusion

In this project I have written computational programs that model the energy band structure of single-walled carbon nanotubes. One of them plots these bands over a single Brillouin zone and allows one to predict the conduction properties of tubes of arbitrary

chirality. It also computes the energies of allowed optical transitions. Another program plots their Brillouin zones in the reciprocal lattice, also for any chirality. This visualization displays the symmetries that lead to degeneracies of energy subbands and the conditions necessary for a tube to be a conductor or a semiconductor. I have shown that a magnetic field parallel to the tube axis shifts these zones, changing its conduction properties, transition energies, and splitting degenerate states. However, it has no effect on the energy bands themselves. Expanding the tight-binding calculation of the graphite band structure to include second nearest neighbor interactions, in contrast, deforms the energy bands slightly but has no effect on the allowed momentum states, or Brillouin zones. The effects of this correction are very small, however. A more complete model would include the effects of excitons, weakly bound hydrogenic electron-hole pairs found in many semiconductors. Experiments have shown that they make significant contributions to the optical spectra. Also of interest would be the lifetime of photogenerated carriers, further analysis of selection rules for optical transitions, and calculations of interband matrix elements.

References

- 1) M. Cardona and P. Yu
Fundamentals of Semiconductors, 3rd edition (Springer-Verlag, 2001)
- 2) M. S. Dresselhaus, G. Dresselhaus, and Ph. Avouris, eds., *Carbon Nanotubes: Synthesis, Structure, Properties, and Applications* (Springer, 2000)
- 3) J. Mintmire and C. T. White, *Carbon* **33**, 893 (1995)
- 4) A. M. Rao and E. Richter, *Science* **275** 187-191 (1997)
- 5) S. Reich, J. Maultzsch, and C. Thomsem. Tight-Binding description of graphene. *Phys. Rev. B* **66** (2002).
- 6) R. Saito, G. Dresselhaus, and M. S. Dresselhaus, *Physical Properties of Carbon Nanotubes* (Imperial College Press, 1998)
- 7) P. R. Wallace, The band theory of graphite. *Phys. Rev.* **71**, 622-634 (1947)